

# Cdon suppresses Vascular Smooth Muscle Calcification via Repression of Wnt/Runx2 axis

Jong-Sun Kang (✉ [kangj01@skku.edu](mailto:kangj01@skku.edu))

Sungkyunkwan University School of Medicine

Byeong-Yun Ahn

Sungkyunkwan University School of Medicine

Su Woo Kim

Department of Molecular Cell Biology, Single Cell Network Research Center

Yideul Jeong

Sungkyunkwan Univeristy

Young-Eun Leem

Department of Molecular Cell Biology, Single Cell Network Research Center, Sungkyunkwan University School of Medicine

---

## Article

**Keywords:** Cdon, vascular calcification, Wnt signaling pathway, vascular smooth muscle cells, osteogenic conversion

**Posted Date:** June 22nd, 2022

**DOI:** <https://doi.org/10.21203/rs.3.rs-1732835/v1>

**License:**  This work is licensed under a Creative Commons Attribution 4.0 International License.

[Read Full License](#)

---

**Version of Record:** A version of this preprint was published at Experimental & Molecular Medicine on January 6th, 2023. See the published version at <https://doi.org/10.1038/s12276-022-00909-7>.

# Abstract

Osteogenic transdifferentiation of vascular smooth muscle cells (VSMCs) is a risk factor associated with vascular diseases. Wnt signaling is one of the major mechanisms implicated in osteogenic conversion of VSMCs. Since Cdon plays a negative role in Wnt signaling in distinct cellular processes, we sought to investigate the role of Cdon in vascular calcification. The expression of Cdon is significantly downregulated in VSMCs of aortas of patients with atherosclerosis and aortic stenosis. Consistently, calcification models including vitamin D3 (VD3)-injected mice and VSMCs cultured with calcifying media exhibited reduced Cdon expression. Cdon ablation mice (cKO) exhibited exacerbated aortic stiffness and calcification in response to VD3, compared to the control. Cdon depletion induced the osteogenic conversion of VSMCs accompanied by cellular senescence. The Cdon-deficient aortas showed a significant alteration in gene expression related to cell proliferation and differentiation together with Wnt signaling regulators. Consistently, Cdon depletion or overexpression in VSMC elevated or attenuated Wnt-reporter activities, respectively. The deletion mutant of second immunoglobulin domain (Ig2) in Cdon ectodomain failed to suppress Wnt signaling and osteogenic conversion of VSMCs. Furthermore, the treatment of purified the recombinant proteins of entire ectodomain or Ig2 domain of Cdon displayed suppressive effects on Wnt signaling and VSMC calcification. Our results demonstrate a protective role of Cdon in VSMC calcification via suppressing Wnt signaling. The Ig2 domain of Cdon has a potential as a therapeutic tool to prevent vascular calcification.

# Introduction

The contractile properties of vascular smooth muscle cells (VSMCs) are critical for the maintenance of vascular function<sup>1</sup>. VSMCs express a variety of contractile proteins such as alpha-smooth muscle actin (αSMA), smooth muscle myosin heavy chain (sm-MHC) and smooth muscle 22α (SM22α) ensuring the contractile function. In response to diverse physiological and pathological stimuli, VSMCs undergo a process called cellular remodeling<sup>2</sup>. In homeostatic remodeling, VSMCs dedifferentiate to proliferate and redifferentiate into muscle cells to regain their contractile properties. Upon pathological insults, VSMCs undergo a phenotypic switch from the contractile to synthetic phenotype and eventually transdifferentiate into osteochondrogenic cell types characterized by the loss of VSMC marker proteins and gain of osteoblast cell marker proteins (such as Runt-related transcription factor 2 (Runx2), osteopontin, etc.)<sup>3,4</sup>. The resulting cells produce mineralizing matrices, and therefore, the osteochondrogenic transdifferentiation of VSMCs is the key event for vascular calcification associated with diverse pathological conditions like aging, diabetes, atherosclerosis, and chronic kidney disease<sup>5-7</sup>. Among multiple signaling pathways, the canonical Wnt signaling is involved in osteogenic transdifferentiation and vascular calcification. In VSMCs, Wnt signaling is activated by the high level of phosphate and induces Runx2 expression, a key transcription factor for the osteochondrogenic transdifferentiation<sup>8,9</sup>. A recent study has demonstrated that the inhibition of Wnt signaling by magnesium reverses the osteogenic conversion of VSMCs<sup>10</sup>. Thus, understanding the regulatory mechanisms of Wnt signaling in VSMCs is important to develop therapeutic strategies against vascular calcification.

Cdon (CAM-related/downregulated by oncogenes) is a member of the immunoglobulin /fibronectin type III superfamily of cell adhesion molecule. Cdon plays critical roles in the development of forebrain and skeletal muscle via regulation of sonic hedgehog (Shh), Wnt, and N-cadherin/cell adhesion signaling<sup>11-13</sup>. A recent study has proposed Cdon as a therapeutic target to promote endothelium integrity in response to acute inflammation via inhibition of desert hedgehog-mediated signaling<sup>14</sup>. In addition to Shh signaling activation by Cdon as a coreceptor, Cdon suppresses Wnt signaling by interacting with LRP6 coreceptor to promote ventral neuronal cell fates in the early forebrain development<sup>15</sup>. A similar suppressive activity of Cdon on Wnt signaling has also been demonstrated in prevention of cardiac remodeling and fibrosis<sup>16</sup>. In consideration of the importance of the fine control of Wnt signaling in vascular system, a question arises whether Cdon plays a role in vascular calcification. The initial open data analysis revealed that Cdon transcripts are declined in calcified aortas, compared to the normal aortas. Consistently, Cdon expression showed a negative correlation with the osteogenic markers (Runx2, Osterix and Osteopontin). Therefore, we generated a tamoxifen (tmx)-inducible SM22 $\alpha$ -Cre<sup>ERT2</sup>; Cdon (Cdon<sup>f/f</sup>) mouse model to ablate Cdon in smooth muscle upon tamoxifen administration. Using these mice, we examined the role of Cdon in vascular calcification induced by vitamin D. Cdon-depletion in VSMCs exacerbated VSMC calcification concurrent with enhanced Wnt signaling. Conversely, Cdon overexpression attenuated the osteogenic conversion of VSMCs via suppressing Wnt signaling. Cdon deletion mutant of the second immunoglobulin domain (Ig2 domain), which is responsible for the Wnt suppressive activity, failed to attenuate the osteogenic conversion of VSMCs. In addition, treatment of purified Ig2-Fc (Ig2 domain fused to Fc domain of human IgG gamma protein) suppressed the calcification of VSMCs. Collectively, these data demonstrate a protective role of Cdon in vascular calcification via suppression of Wnt signaling. Furthermore, the Ig2 domain of Cdon has a great potential as a therapeutic agent to intervene vascular calcification.

## Materials And Methods

### Animal studies

Mice bearing Cdon-floxed allele (Cdon<sup>f/f</sup>) were obtained from EUCOMM and maintained as previously described<sup>17</sup>. For Cdon deletion in vascular muscle cells, Cdon<sup>f/f</sup> mice were crossed with SM22 $\alpha$ -Cre<sup>ERT2</sup> mice which express tamoxifen-inducible Cre recombinase under the transcriptional control of the SM22 $\alpha$  (Tagln, smooth muscle protein 22-alpha) promoter. SM22 $\alpha$ -Cre<sup>ERT2</sup> mice were obtained from Severance Integrative Research Institute for Cerebral & Cardiovascular Diseases (SIRIC, Yonsei University Health System). To induce the deletion of one of the exons of Cdon gene in VSMCs, around 8 weeks old mice were injected intraperitoneally with 100 mg/kg tamoxifen (tmx, Sigma-Aldrich) every two days for five times. To generate the model of vascular calcification in mice, 8 weeks old C57BL/6 male mice and vehicle or tamoxifen-injected mice were administrated by vitamin D3 (VD3, 5x10<sup>5</sup> IU/kg per day; Cayman Chemical). 14.575 mg VD3 in 70 ml of ethanol was mixed with 500 ml Cremophor for 15 min at room temperature, and this solution was then mixed with 6.2 ml sterilized water including 250 mg of dextrose

for 15 min at room temperature. The mice were injected with a dose of VD3 (150 ml/25 g per day) subcutaneously for consecutive 3 days<sup>18</sup>.

The animal experiments in this study were approved by the Institutional Animal Care and Use Committee (IACUC) of Sungkyunkwan University School of Medicine (SUSM) and complied with the animal experiments guidelines of the SUSM Ethics Committee (the protocol number: SKKUIACUC 2020-04-14-1).

## Echocardiography

To measure the cardiac function and the pulse wave velocity (PWV), echocardiographic analysis was performed 1 day before sacrifice. Mice were anesthetized with 1-2 % (vol/vol) isoflurane and body temperature was maintained at 36-38 °C with a heating lamp and a heating platform. Heart rates are monitored and generally maintained at 400-500 beats per minute. Echocardiography was carried out using a Vevo LAZR-X machine (the BIORP of Korea Basic Science Institute) with a 40-MHz probe (visual sonic). Analysis of M-mode images derived from the short-axis view of the left ventricle was carried out to measure the ejection fraction (EF) and the fractional shortening (FS)<sup>19</sup>. PWV was obtained from the B-mode and pulse-waved (PW) doppler mode of aortic arch view, calculated as  $PWV = \text{Aortic arch distance} / \text{transit time (cm/s)}$ . The PW doppler mode sample volume was placed in the ascending aorta and the time (T1) from the onset of the QRS complex to the onset of the ascending aortic Doppler waveform was measured. On the same image plane, the PW doppler mode sample volume was placed as distal as possible in the descending aorta and the time (T2) from the onset of the QRS complex to the onset of the ascending aortic Doppler waveform was measured. Obtained values for T1 and T2 were averaged over 10 cardiac cycles. The aortic arch distance was measured between the 2 sample volume positions along the central axis of the aortic arch on the B-mode image, and the transit time was calculated by  $T2 - T1$  (ms)<sup>20</sup>.

## Cell culture

A7R5 (ATCC, CRL-1444) cells were cultured in normal media containing DMEM, 10% FBS, and 1% P/S as previously described<sup>21</sup>. For inducing the vascular calcification *in vitro*, the cells incubated with normal media were switched to calcifying media (CM) for up to 3 days or 7 days. The media were replenished every 48 h and the first day of culture in CM was defined as day 0. CM was generated by adding 100nM dexamethasone, 1mM insulin, 50mg/ml ascorbic acid, 10mM b-glycerophosphate, and 8mM CaCl<sub>2</sub> to normal media<sup>18</sup>. Transfection experiments were performed by utilizing 1mg/ml polyethylenimine (PEI, Sigma-Aldrich). To analyze the effects of Cdon on Wnt signaling, cells were treated with 20ng/ml Wnt3a (R&D systems) and 4mM XAV939 (Calbiochem). To deplete the expression of Cdon in A7R5, control shRNA (shcont) or Cdon shRNA (shCdon) were expressed by using lentiviral expression system as previously described<sup>17</sup>.

## Histological analysis

Aortas were isolated from PBS perfused mice and fixed with 4% PFA, embedded in paraffin, and sectioned with 5 mm thickness. For determination of calcium deposition in aortas, slide sections were stained with Von Kossa stain. Briefly, deparaffinized sections were incubated with 1% silver nitrate solution under ultraviolet for 2 h followed by the step removing unreacted silver with 5% sodium thiosulfate for 5 min. Sections were counterstained with nuclear fast red for 5 min before dehydration and mounting<sup>18</sup>. To quantify the amount of calcium deposition in aortas, the images obtained from TissueFAXS PLUS (TISSUEGNOSTICS) were analyzed in ImageJ software (NIH).

## **Immunofluorescence**

For the immunohistochemistry in aorta samples, deparaffinized samples were boiled in Tris-EDTA buffer (pH9.0, 0.05% Tween-20) for the antigen retrieval followed by the standard protocol. To analyze the cell death during vascular calcification, Click-iT TUNEL assay Alexa imaging assay kit (Invitrogen, C10246) was utilized on cryosections of aortas which were isolated from PBS perfused mice and sectioned with 5mm thickness. Fluorescence images were analyzed with an LSM-710 confocal microscope (Carl Zeiss) as previously described<sup>16</sup>.

## **Protein and RNA analysis**

Immunoblot analysis was carried out as previously described<sup>16</sup>. In brief, cultured cells and homogenized tissues of aortas were lysed in RIPA buffer (protease inhibitor cocktail [Roche, 1183617001], pH8.0; 150mM NaCl; 1mM EDTA; 1% Triton X-100; 10mM Tris-HCl). The primary antibodies used in this study are listed in Supplementary table 1.

Quantitative RT-PCR and RNA sequencing analysis were performed as previously described<sup>16</sup>. Total RNAs from cells and homogenized tissues were extracted with easy-BLUE (iNtRON) reagent following the manufacturer's instruction. cDNA samples were generated from 0.5 mg of RNAs by PrimeScript RT reagent (TaKaRa) according to the manuscript's protocol. The primer sequences used in this study are listed in Supplementary table 2. High-throughput sequencing was performed as single-end 75 sequencings using Illumina NExtSeq 500 (ebiogen, Korea). The analysis for RNA sequencing data was performed by using ExDEGA v3.2 (ebiogen) and a heatmap was displayed utilizing Morpheus (<http://software.broadinstitute.org/morpheus/>). The global gene expression was assessed by the reactome with Gene Set Enrichment Analysis (GSEA) (<http://www.gsea-msigdb.org/gsea/msigdb/index.jsp>) using MsigDB database v7.2 (>1.3 fold, |RC log2|>2, p<0.05).

The aortic transcriptomes of human from the NCBI Gene Expression Omnibus (GEO; <http://www.ncbi.nlm.nih.gov/geo>) database (GSE43292, GSE12644, and GSE83453) were computed for the analysis of gene expression and Pearson's correlations with the Graphpad PRISM7. The single-cell transcriptome of human patients (GSE159677) was utilized for extracting each cell type in aortas including VSMCs, endothelial cells, macrophages, T-lymphocytes, B-lymphocytes, and NK-cells by marker genes. The genes of VSMCs were aligned and projected through Uniform manifold approximation and

projection (UMAP) to explore the scRNA-seq data. Visualization of gene expression was carried out in Graphpad PRISM7.

Luciferase reporter assay was performed as previously described<sup>15</sup>. Briefly, A7R5 cells were transfected with control or Cdon overexpressing or siCdon plasmids, b-catenin-responsive Top-Flash luciferase construct plasmid. Cells were analyzed for luciferase activity with a microplate luminometer according to manufactures protocol 24 h after transfection (Promega).

### **Alizarin Red stain**

Cells were washed with PBS and fixed with 4% PFA for 15 min at room temperature. Cells were then washed twice with deionized water and covered with 40mM Alizarin Red S (Sigma-Aldrich) at around pH4.2 for 2 h at room temperature with gentle shaking. To remove the unstained dye, cells were washed thrice with deionized water before images were obtained using Nikon CELIPS TE-2000U. To quantify the amount of calcification, Alizarin Red S was extracted with 10% acetic acid for 30 min at room temperature, scraped into a microcentrifuge tube, vortexed, and incubated at 85 °C for 15 min. After chilling on ice for 5 min, the mixture was centrifuged at 20,000 g for 15 min at 4 °C. The supernatant was transferred to a new tube and 10% ammonium hydroxide was added to the supernatant. Absorbance was read in triplicate at 405 nm using a 96-well plate spectrophotometer<sup>18</sup>.

### **Protein purification**

HEK293T cells were transfected with recombinant proteins of Cdon fused with the Fc region of human IgG gamma listed as follows: Cdon-Fc; the entire ectodomain fused to Fc, Ig2-Fc; Fc fusion protein with Ig2 domain<sup>15</sup>. At 72 h after transfection, cells were pelleted by centrifugation at 2,000 g for 10 min. The supernatant was then filtered (0.45 mm), followed by a standard protocol for Protein A antibody purification<sup>22</sup>. In briefly, the supernatant was incubated with Protein A agarose (Millipore) for 1 h at room temperature under constant rotation. Bound proteins were eluted with 0.1M citric acid (pH 3.0) and immediately neutralized with 1M Tris-HCl (pH 8.0). Eluates were concentrated using Amicon Ultra-4 centrifugal filters (MWCO 3K, EMD Millipore) and dialysed against PBS. Protein concentrations were determined using A280 measurements. Protein purity and integrity was assessed by SDS-PAGE.

### **Statistical analysis**

Values are means  $\pm$ SEM or SD as noted. Statistical significance was calculated by paired or unpaired Student's t-test or one-tailed Analysis of variance (ANOVA) test followed by Tukey's test (GraphPad Prism software, v7). Differences were considered as significant at  $p < 0.05$ .

## **Results**

### **Cdon expression is reduced in calcified aorta and VSMCs during osteogenic conversion**

The immunostaining data of mouse aorta revealed the expression of *Cdon* in the medial smooth muscle region, as well as in intimal endothelial cell regions (**Supplementary Fig. 1a**). Next, we analyzed the datasets (GSE43292, GSE12644, and GSE83453) obtained from aorta isolated from patients with atherosclerosis and stenosis for *Cdon* expression, together with aortic calcified markers such as *Runx2*, Alkaline phosphatase (ALPL), and CD68 (**Supplementary Fig. 1b**). *Cdon* is significantly downregulated in atherosclerotic plaque and calcified aorta (**Fig. 1a**), while the other coreceptors of Shh such as *Boc* and *Gas1* are not significantly altered (**Supplementary Fig. 1b**). To further examine the expression pattern of *Cdon* in each cell type of aortas, we examined scRNA data (GSE159677) obtained from calcified atherosclerotic plaques (AC) and proximal adjacent portions (PA) of three patients (**Fig. 1b**). The single-cell transcriptome analysis revealed a decrease in *Cdon* expression in VSMCs as well as endothelial cells, and macrophages (**Fig. 1c** and **Supplementary Fig. 1c**). Taken together, these data implicate the potential role of *Cdon* in VSMCs during vascular pathogenesis.

We went on to investigate the role of *Cdon* in vascular calcification by using vascular calcification mouse model generated by subcutaneous administration of vitamin D3 (VD3) for consecutive 3 days (**Supplementary Fig. 2a**). The treatment of VD3 for 3 days induced aortic stiffness without overt cardiac dysfunction (**Supplementary Fig. 2b**). In the VD3-injected aortas, the osteogenic conversion was evident by the increase in osteogenic genes such as *Runx2* and the calcified area stained by Von Kossa. However, the expression of foam cell markers such as CD146 and CD68 was not significantly altered (**Supplementary Fig. 2c, d**). Consistent with the open data analysis, calcified aortas induced by VD3 had decreased levels of *Cdon* transcript and protein, relative to control aortas (**Fig. 1d-f**). To further assess the effect of calcification on *Cdon* expression, A7R5 VSMCs were treated with calcifying medium (CM) to mimic *in vivo* calcification (**Supplementary Fig. 2e, f**). Similar to the *in vivo* calcification model, CM treatment also reduced *Cdon* expression, while elevating the expression osteogenic markers such as *Runx2* and ALPL (**Fig. 1g, h** and **Supplementary Fig. 2g**). Collectively, these data suggest a potential role of *Cdon* in the prevention of vascular calcification.

### VSMC-*Cdon* ablation in mice exacerbates vitamin D3-induced aortic calcification

Next, we examined the effect of *Cdon* deficiency on VD3-induced vascular calcification by using smooth muscle-specific *Cdon* ablated mice. We generated mice bearing tamoxifen (tmx)-inducible Cre-recombinase under the control of VSMC-specific SM22a promoter (*Cdon*<sup>f/f;SM22a-Cre-ERT2</sup>). Smooth muscle-specific deletion of *Cdon* (cKO) was induced by intraperitoneal injection of tmx for five times with 2 days interval (**Supplementary Fig. 3a**). *Cdon* protein levels were decreased in cKO aortas, while other cKO tissues did not display any changes in *Cdon* levels, compared to WT tissues (**Supplementary Fig. 3b, c**). The residual *Cdon* proteins in aorta might be from other cell types like endothelial cells. To induce vascular calcification, VD3 was subcutaneously administrated to mice for 3 days post 1 week of tmx injection (**Fig. 2a**). While *Cdon* deletion alone did not induce vascular calcification, it aggravated the aortic stiffness in response to VD3 injection without cardiac dysfunction (**Fig. 2b** and **Figure S4**). The calcified area induced by VD3 was also increased in cKO, compared to f/f mice (**Fig. 2c, d**). The expression of *Runx2* and ALPL was elevated by the VD3 injection in both control and cKO aortas, but it was elevated to

a greater degree in the VD3-injected cKO aortas (**Fig. 2e**). cKO aortas also displayed greater number of cell deaths triggered by VD3 injection compared to the WT aortas, evident by TUNEL-positive cells (**Fig. 2c, f**). Collectively, these data show that Cdon deletion in VSMCs exacerbates vascular calcification.

### **Cdon depletion induces osteogenic transdifferentiation of VSMCs**

To further verify the effect of Cdon depletion in smooth muscle cells, A7R5 cells were transduced by control or Cdon shRNA expressing lentiviruses and subjected to calcification analysis. Interestingly, Cdon depletion alone elevated the level of Runx2 proteins and the alizarin red staining intensity without calcification induction (**Fig. 3a-c**). Similarly, Cdon depletion induced the increase in transcript levels of osteogenic markers such as Runx2 and ALPL, while the gene expression related to foam cell markers were not significantly altered relative to the control infected cells (**Fig. 3d**). The osteogenic increase in Cdon-depleted cells without calcification triggers might be due to the stresses caused by lentiviral infection. Since control virus infection did not show any signs of calcification in A7R5 cells, Cdon depletion might sensitize VSMCs to other stresses to trigger calcification. These data imply that Cdon plays a critical role in the maintenance of VSMC characteristics. Previous studies have shown that cellular senescence is a prominent driver for vascular dysfunction<sup>23</sup>. A recent study has shown that Cdon ablation in skeletal muscle stem cells augments cellular senescence upon muscle injury leading to impaired muscle regeneration<sup>17</sup>. Thus, we assessed whether Cdon depletion causes cellular senescence of VSMCs by using senescence associated b-galactosidase (SA-b-gal) staining. Cdon-depleted VSMC cells had about 3.5-fold increase in SA-b-gal positive cells, relative to control cells (**Fig. 3e, f**). The expression of senescence markers such as p16 and p21 was also increased in Cdon-depleted VSMCs (**Fig. 3g**). Taken together, these data suggest that Cdon depletion facilitate osteogenic conversion and cellular senescence of VSMCs.

### **Cdon deficiency in aortas results in alterations of genes related to immune response, cell death, cell to cell adhesion and Wnt signaling**

To analyze Cdon-mediated molecular mechanisms in vascular calcification, we performed RNA sequencing with WT and cKO aortas at 1 day after VD3 injection (**Fig. 4a**). There were 373 differentially expressed genes (DEGs) in VD3-treated WT (WV) vs vehicle-treated WT (WC), and 299 DEGs in VD3 treated cKO (KV) vs WV (>1.3-fold, average of normalized RC log<sub>2</sub>>2, p-value <0.05 with biological repeat, **Fig. 4b**). There were 24 DEGs that overlapped between WV vs WC and KV vs WV, and we hypothesized that those genes are not Cdon-related genes. Thus, each DEG in WV vs WC or KV vs WV excluding the overlapping genes was further analyzed by using Gene Set Enrichment Analysis (GSEA) (**Fig. 4c**). The data revealed that genes related to immune response, cell death, and cell to cell adhesion were significantly altered only in WV vs WC, while genes implicated in cell proliferation, cell differentiation, and gene expression regulation were altered in KV vs WV (**Fig. 4c, d**). Notably, in KV vs WV, genes related to Wnt signaling regulation such as Cytoplasmic activation/proliferation-associated protein 2 (*Caprin2*), Wnt inhibitory factor 1 (*Wif1*), and *Wnt9a* were altered. Consistently, Cdon-deficient aortas exhibited altered Wnt activities in response to VD3 (**Fig. 4e**), which were further confirmed by quantitative RT-PCR analysis

(**Fig. 4f**). To further examine the relationship between Cdon and Wnt signaling, we assessed the aortic transcriptome from patients suffering from atherosclerosis and aortic stenosis (GSE43292, GSE12644, and GSE83453) (**Supplementary Fig. 5a**). We found a negative correlation between Cdon and Wnt target genes including *Wnt3*, *Ctnnb1*, *Fzd1*, and *Axin2* (**Supplementary Fig. 5b**). Taken together, these data suggest that Cdon deficiency causes changes in VSMC proliferation and differentiation via Wnt signaling.

### **Cdon depletion enhances Wnt signaling leading to VSMC calcification**

To further examine the interaction of Cdon with Wnt signaling in vascular calcification, we assessed the expression of a Wnt target gene *Axin2* in Cdon-deleted aortas. *Axin2* transcript level was significantly elevated in both WT and cKO aortas treated with VD3, but significantly higher in cKO aorta (**Fig. 5a**). Consistently, Cdon-depletion in VSMCs caused a significant increase in *Axin2* expression compared to the control (**Fig. 5b**). The level of b-Catenin was also substantially elevated in Cdon-depleted VSMCs (**Fig. 5c**). Furthermore, the activity of Topflash Wnt-reporter was elevated in Cdon-depleted VSMCs compared to the control, and the difference between the Cdon-depleted VSMCs and the control became more prominent in response to Wnt3a (**Fig. 5d**). In contrast, Cdon overexpression reduced Wnt reporter activities and *Axin2* expression in both basal and Wnt3a-treated conditions (**Fig. 5e, g**). Furthermore, Cdon overexpression attenuated the increase in b-Catenin and Runx2 proteins in response to Wnt3a, compared to control cells (**Fig. 5f**). Taken together, these data suggest that Cdon modulates Wnt signaling activation in VSMCs.

### **Cdon overexpression attenuates the CM-induced osteogenic conversion of VSMCs**

Since Cdon expression is decreased in calcified VSMCs, we examined whether Cdon overexpression attenuates CM-induced osteogenic conversion. Cdon-overexpressing VSMCs exhibited reduced levels of Runx2 and b-catenin proteins in response to CM (**Fig. 6a**). In addition, CM treatment significantly elevated Wnt-reporter activity, which was attenuated by Cdon overexpression (**Fig. 6b**). Cdon overexpression also blunted the expression of *Axin2*, Runx2, and ALPL in response to CM (**Fig. 6c**). Consistently, Cdon overexpression inhibited CM-induced osteogenic transdifferentiation of VSMCs (**Fig. 6d, e**). Taken together, these data suggest that Cdon overexpression suppresses Wnt signaling and VSMC calcification.

### **Cdon attenuates the osteogenic conversion by inhibition of Wnt signaling**

We have previously reported that Cdon suppresses Wnt signaling through interaction with a Wnt coreceptor LRP6 mediated by its second immunoglobulin domain (Ig2)<sup>15</sup>. Thus, we have examined the effect of wildtype Cdon (WT) and a deletion mutant for the second Ig domain (DIg2) on the CM-mediated osteogenic conversion. Unlike the suppressive effect of WT on b-Catenin level in response to CM, DIg2 mutant failed to fully repress the induction of b-catenin and Runx2 levels (**Fig. 7a**). In addition, DIg2 mutant failed to blunt *Axin2* expression which is greatly elevated by CM but attenuated by WT expression (**Fig. 7b**). Furthermore, the inhibitory effect on the CM-induced osteogenic conversion of VSMCs was smaller by the DIg2 mutant expression compared to the WT expression (**Fig. 7c, d**). In consistence with previous results, WT overexpression attenuated the increase in b-catenin and Runx2 by Wnt3a treatment, while DIg2 expression failed to suppress this increase (**Fig. 7e**). Similarly, *Axin2* increase induced by

Wnt3a was abrogated by WT while Dlg2 mutant failed to fully suppress it (**Fig. 7f**). Consistently, WT overexpression reduced Wnt3a-induced osteogenic conversion while Dlg2 expression failed to do so (**Fig. 7g, h**). Collectively, these data imply that Cdon plays a preventive role of VSMC calcification through Wnt inhibition.

### **Cdon-Ig2/Fc fusion protein exhibits a preventive effect against VSMC calcification**

Next, we further examined the effect of the secreted recombinant proteins of Cdon ectodomain (Cdon-Fc) or Ig2 domain (Ig2-Fc) fused to the Fc domain of human IgG gamma. The expression of recombinant proteins was validated in supernatants of cells transfected with Cdon-Fc or Ig2-Fc by immunoblot analysis (**Fig. 8a**). The treatment of purified Cdon-Fc or Ig2-Fc (10 mg/ml) in VSMCs also blocked CM-induced b-catenin activation and Runx2 induction, compared to human IgG as the negative control (**Fig. 8b**). CM-induced osteogenic conversion was also attenuated by Cdon-Fc or Ig2-Fc, but not by control human IgG (**Fig. 8c, d**). Furthermore, Cdon-Fc or Ig2-Fc treatment attenuated CM-induced Axin2, Runx2 and ALPL expression while control IgG did not show any effect (**Fig. 8e**). Taken together, these data suggest that Ig2 domain of Cdon is sufficient to suppress Wnt signaling and VSMC calcification. In summary, Cdon plays a critical role for Wnt signaling suppression thereby preventing vascular calcification.

## **Discussion**

Our data demonstrate a critical role of Cdon in vascular calcification. The transcriptome data from aorta isolated from patients with atherosclerosis and stenosis revealed a significant decrease in Cdon levels in VSMCs. In agreement, Cdon was reduced in aortas of VD3-induced vascular calcification mouse models or in VSMCs treated with CM. Furthermore, Cdon ablation in vascular smooth muscles exacerbated VD3-induced vascular calcification. Therefore, Cdon is an important regulator for vascular remodeling.

Shh signaling induces the proliferation of VSMCs, an essential step for intimal hyperplasia and the pathogenesis of vascular diseases<sup>24</sup>. Since Cdon activates Shh signaling as a coreceptor<sup>25</sup>, we have initially predicted that Cdon depletion might reduce the proliferation of VSMCs and vascular remodeling via reduced Shh signaling. The transcriptome analysis revealed alterations in genes related to cell proliferation as well as differentiation in Cdon-deficient aortas treated with VD3. However, the involvement of Shh signaling in vascular calcification of Cdon-deficient aorta is unclear. Genes related Shh signaling were not greatly altered in Cdon deficient aorta in response to VD3. Unlike the reduced expression of Cdon, the expression of other Shh signaling components, Boc, Gas1, and Shh, was also not significantly changed in the transcriptome data from aorta isolated from patients with atherosclerosis and stenosis. Furthermore, Cdon depletion increased cellular senescence and death in the medial region of aorta in response to VD3-mediated calcification. These data support for an independent role of Cdon from Shh signaling in vascular diseases.

BMP signaling plays a critical role in osteogenic differentiation of VSMCs<sup>26,27</sup>. BMP2, one of the transforming growth factors (TGF)- $\beta$  family, activates Runx2 in diverse cell types including VSMCs and plays a crucial role in bone repair<sup>28,29</sup>. Aortic transcriptome analysis revealed a negative correlation between Cdon and BMP signaling pathway. However, there was no significant difference in BMP signaling in Cdon-overexpressing or depleted VSMCs by reporter assay (data not shown). Thus, BMP signaling also seems to be not directly involved in Cdon-mediated VSMC regulation.

In addition to BMP signaling, an inverse correlation between Cdon and Wnt target genes was observed in aortic transcriptome of patients with atherosclerosis and stenosis. Wnt signaling is another major mechanism implicated in osteogenic conversion of VSMCs. In line with the negative effects of Cdon on Wnt signaling in forebrain development<sup>15</sup>, Cdon deficiency in VSMCs resulted in Wnt signaling dysregulation and enhanced osteogenic conversion. Our previous study has identified the second Ig region of the ectodomain of Cdon to be responsible for Wnt signaling suppression by interacting with LRP6<sup>15</sup>. Accordingly, the deletion of Ig2 in Cdon failed to block the osteogenic conversion in response to calcifying medium or Wnt3a treatment, suggesting a requirement of Wnt inhibition by Ig2 domain to prevent VSMC conversion. Consistently, the Fc fusion protein of Ig2 domain exhibited a suppressive activity of Wnt signaling and a protective effect on vascular calcification. Thus, Cdon represents a potential therapeutic tool for vascular calcification via suppression of Wnt signaling activity. Since Wnt signaling pathway is involved in diverse diseases including cancers and neurodegenerative diseases, the regulatory mechanisms of Wnt signaling are continuously investigated for the development of therapeutic strategies<sup>30-32</sup>. DKK (Dickkopf) proteins, the Wnt regulatory molecules, bind to LRP5/6 coreceptors, thereby acting as functional antagonists of Wnt signaling<sup>33</sup>. Interestingly, inhibition of Wnt signaling by DKK plays a complex role in cardiovascular diseases. DKK1 is elevated in plasma and lesions of patients with atherosclerosis and type 2 diabetes with cardiovascular diseases<sup>34,35</sup>. Excessive DKK1 can promote endothelial cell dysfunction associated with increased inflammation, likely contributing to atherosclerosis<sup>36</sup>. On the other hand, DKK1 can attenuate calcium deposition and expression of RUNX2 in calcified aortas from chronic kidney disease, in a similar manner to Cdon<sup>37</sup>. The opposing effects of DKK1 may be attributed to the distinct role dependent on the cellular context and the protein's Wnt-independent signaling activities. A recent study on Cdon in endothelium has reported its role as a negative regulator of desert hedgehog-driven endothelial integrity in inflammation conditions<sup>14</sup>. Therefore, therapeutic strategies using Wnt signaling regulators will require high specificity to avoid undesirable outcomes. In case of Cdon, its interaction with hedgehog proteins is mediated by the third fibronectin domain<sup>38</sup>. Since Ig2 domain of Cdon has shown to be sufficient to distinctively target and suppress Wnt signaling activities, the use of the Ig2 domain of Cdon may serve as a specific suppressor of Wnt signaling pathway while avoiding intervention with other signaling pathways.

Accumulating evidence suggests that cellular senescence is closely linked with the vascular pathogenesis<sup>23,39</sup>. Cellular senescence of VSMC has been associated with the induction of osteogenic markers including Runx2 and ALPL<sup>40</sup>. Thus, cellular senescence is considered as a major risk factor for

vascular calcification. Cdon deficient VSMCs exhibit increased cellular senescence in response to calcification stress. Similarly, skeletal muscle stem cells deficient for Cdon display cellular senescence contributing to regeneration impairment<sup>17</sup>. The mechanism by which Cdon depletion causes cellular senescence is currently unclear. Decreased Wnt activity has been generally linked with cellular senescence<sup>41</sup>, but a recent study has reported that canonical Wnt signaling pathway in chondrocytes induces cellular senescence associated with inflammation<sup>42</sup>. Further study is required to elucidate the exact role of Wnt signaling and Cdon in VSMC senescence. Hereof, we report the suppressive effects of Ig2 domain of Cdon on Wnt signaling pathway via interacting LRP6, implicating that Ig2 domain of Cdon could be a good candidate for the therapeutic strategy in vascular diseases.

## Declarations

### Acknowledgements

Authors are also grateful to Jin-Woo Lee for the critical comments and reading of manuscript. This research was supported by the National Research Foundation Grant funded by the Korean Government (MIST) (NRF-2022R1A2B5B02001482; NRF-2016R1A5A2945889).

### Conflict of interest

The authors declare that they have no conflict of interest.

### Author contributions

B.Y.A, S.K., Y.J., Y.E.L. and J.S.K. conceived the experimental design and performed the experiments. B.Y.A. and J.S.K. analyzed and interpreted of the results and carried out the statistical analysis. B.Y.A. and J.S.K. wrote the manuscript.

## References

1. Steucke, K.E., Tracy, P.V., Hald, E.S., Hall, J.L. & Alford, P.W. Vascular smooth muscle cell functional contractility depends on extracellular mechanical properties. *J Biomech.* **48**, 3044-3051 (2015).
2. Shi, N., Mei, X. & Chen, S.Y. Smooth muscle cells in vascular remodeling. *Arterioscler Thromb Vasc Biol.* **39**, e247-e252 (2019).
3. Petsophonsakul, P. *et al.* Role of vascular smooth muscle cell phenotypic switching and calcification in aortic aneurysm formation. *Arterioscler Thromb Vasc Biol.* **39**, 1351-1368 (2019).
4. Durham, A.L., Speer, M.Y., Scatena, M., Giachelli, C.M. & Shanahan, C.M. Role of smooth muscle cells in vascular calcification: implications in atherosclerosis and arterial stiffness. *Cardiovasc Res.* **114**, 590-600 (2018).
5. Vazquez-Padron, R.I. *et al.* Aging exacerbates neointimal formation, and increases proliferation and reduces susceptibility to apoptosis of vascular smooth muscle cells in mice. *J Vasc Surg.* **40**, 1199-

- 1207 (2004).
6. Yahagi, K. *et al.* Pathology of human coronary and carotid artery atherosclerosis and vascular calcification in diabetes mellitus. *Arterioscler Thromb Vasc Biol.* **37**, 191-204 (2017).
  7. Dusing, P. *et al.* Vascular pathologies in chronic kidney disease: pathophysiological mechanisms and novel therapeutic approaches. *J Mol Med (Berl).* **99**, 335-348 (2021).
  8. Voelkl, J. *et al.* Signaling pathways involved in vascular smooth muscle cell calcification during hyperphosphatemia. *Cell Mol Life Sci.* **76**, 2077-2091 (2019).
  9. Cai, T. *et al.* WNT/beta-catenin signaling promotes VSMCs to osteogenic transdifferentiation and calcification through directly modulating Runx2 gene expression. *Exp Cell Res.* **15**, 206-217 (2016).
  10. Montes de Oca, A., *et al.* Magnesium inhibits Wnt/beta-catenin activity and reverses the osteogenic transformation of vascular smooth muscle cells. *PLoS One.* **9**, e89525 (2014).
  11. Sanchez-Arrones, L., Cardozo, M., Nieto-Lopez, F. & Bovolenta, P. Cdon and Boc: Two transmembrane proteins implicated in cell-cell communication. *Int J Biochem Cell Biol.* **44**, 698-702 (2012).
  12. Bae, G.U. *et al.* Mutations in CDON, encoding a hedgehog receptor, result in holoprosencephaly and defective interactions with other hedgehog receptors. *Am J Hum Genet.* **89**, 231-240 (2011).
  13. Cole, F., Zhang, W., Geyra, A., Kang, J.S. & Krauss, R.S. Positive regulation of myogenic bHLH factors and skeletal muscle development by the cell surface receptor CDO. *Dev Cell.* **7**, 843-854 (2004).
  14. Chapouly, C. *et al.* Desert hedgehog-driven endothelium integrity is enhanced by Gas1 (Growth Arrest-specific 1) but negatively regulated by Cdon (Cell Adhesion Molecule-Related/Downregulated by Oncogenes). *Arterioscler Thromb Vasc Biol.* **40**, e336-e349 (2020).
  15. Jeong, M.H. *et al.* Cdo suppresses canonical Wnt signalling via interaction with LRP6 thereby promoting neuronal differentiation. *Nat Commun.* **5**, 5455 (2014).
  16. Jeong, M.H. *et al.* Cdon deficiency causes cardiac remodeling through hyperactivation of Wnt/beta-catenin signaling. *Proc Natl Acad Sci U S A.* **114**, e1345-e1354 (2017).
  17. Bae, J.H. *et al.* Satellite cell-specific ablation of Cdon impairs integrin activation, FGF signalling, and muscle regeneration. *J Cachexia Sarcopenia Muscle.* **11**, 1087-1103 (2020).
  18. Kwon, D.H. *et al.* MDM2 E3 ligase-mediated ubiquitination and degradation of HDAC1 in vascular calcification. *Nat Commun.* **7**, 10492 (2016).
  19. Ahn, B.Y. *et al.* PRMT7 ablation in cardiomyocytes causes cardiac hypertrophy and fibrosis through beta-catenin dysregulation. *Cell Mol Life Sci.* **79**, 99 (2022).
  20. Lee, L. *et al.* Aortic and cardiac structure and function using high-resolution echocardiography and optical coherence tomography in a mouse model of Marfan Syndrome. *PLoS One.* **11**, e0164778 (2016).
  21. Pyun, J.H. *et al.* Inducible PRMT1 ablation in adult vascular smooth muscle leads to contractile dysfunction and aortic dissection. *Exp Mol Med.* **53**, 1569-1579 (2021).
  22. Hober, S., Nord, K. & Linhult, M. Protein A chromatography for antibody purification. *J Chromatogr B Analyt Technol Biomed Life Sci.* **848**, 40-47 (2007).

23. Chi, C. *et al.* Vascular smooth muscle cell senescence and age-related disease: state of the art. *Biochim Biophys Acta Mol Basis Dis.* **1865**, 1810-1821 (2019).
24. Li, F. *et al.* Sonic hedgehog signaling induces vascular smooth muscle cell proliferation via induction of the G1 cyclin-retinoblastoma axis. *Arteriosclero Thromb Vasc Biol.* **30**, 1787-1794 (2010).
25. Jeong, M.H. *et al.* A Shh coreceptor Cdo is required for efficient cardiomyogenesis of pluripotent stem cells. *J Mol Cell Cardiol.* **93**, 57-66 (2016).
26. Zhu, D. *et al.* BMP-9 regulates the osteoblastic differentiation and calcification of vascular smooth muscle cells through an ALK1 mediated pathway. *J Cell Mol Med.* **19**, 165-174 (2015).
27. Zebboudj, A.F., Shin, V. & Bostrom, K. Matrix GLA protein and BMP-2 regulate osteoinduction in calcifying vascular cells. *J Cell Biochem.* **90**, 756-765 (2003).
28. Li, X., Yang, H.Y. & Giachelli, C.M. BMP-2 promotes phosphate uptake, phenotypic modulation, and calcification of human vascular smooth muscle cells. *Atherosclerosis.* **199**, 271-277 (2008).
29. Nahar-Gohad, P., Gohad, N., Tsai, C.C., Bordia, R. & Vyavahare, N. Rat aortic smooth muscle cells cultured on hydroxyapatite differentiate into osteoblast-like cells via BMP-2-SMAD-5 pathway. *Calcif Tissue Int.* **96**, 359-369 (2015).
30. Foulquier, S. *et al.* WNT signaling in cardiac and vascular disease. *Pharmacol Rev.* **70**, 68-141 (2018).
31. A Najafi, S.M.A. The canonical Wnt signaling (Wnt/beta-catenin pathway): a potential target for cancer prevention and therapy. *Iran Biomed.* **24**, 269-280 (2020).
32. Libro, R., Bramanti, P. & Mazzon, E. The role of the Wnt canonical signaling in neurodegenerative diseases. *Life Sci.* **158**, 78-88 (2016).
33. Baetta, R. & Banfi, C. Dkk (Dickkopf) proteins. *Arterioscler Thromb Vasc Biol.* **39**, 1330-1342 (2019).
34. Zeng, P. *et al.* ERK1/2 inhibition reduces vascular calcification by activating miR-126-3p-DKK1/LRP6 pathway. *Theranostics.* **11**, 1129-1146 (2021).
35. Garcia-Martin, A. *et al.* Relationship of Dickkopf1 (DKK1) with cardiovascular disease and bone metabolism in Caucasian type 2 diabetes mellitus. *PloS One.* **9**, e111703 (2014).
36. Ueland, T. *et al.* Dickkopf-1 enhances inflammatory interaction between platelets and endothelial cells and shows increased expression in atherosclerosis. *Arterioscler Thromb Vasc Biol.* **29**, 1228-1234 (2009).
37. Fang, Y. *et al.* CKD-induced wntless/integration1 inhibitors and phosphorus cause the CKD-mineral and bone disorder. *J Am Soc Nephrol.* **25**, 1760-1773 (2014).
38. Tenzen, T. *et al.* The cell surface membrane proteins Cdo and Boc are components and targets of the Hedgehog signaling pathway and feedback network in mice. *Dev Cell.* **10**, 647-656 (2006).
39. Ungvari, Z., Tarantini, S., Donato, A.J., Galvan, V. & Csiszar, A. Mechanisms of vascular aging. *Circ Res.* **123**, 849-867 (2018).
40. Nakano-Kurimoto, R. *et al.* Replicative senescence of vascular smooth muscle cells enhances the calcification through initiating the osteoblastic transition. *Am J Physiol Heart Circ Physiol.* **297**, H1673-1684 (2009).

41. Ye, X. *et al.* Downregulation of Wnt signaling is a trigger for formation of facultative heterochromatin and onset of cell senescence in primary human cells. *Mol Cell.* **27**, 183-196 (2007).
42. Li, W., Xiong, Y., Chen, W. & Wu, L. Wnt/beta-catenin signaling may induce senescence of chondrocytes in osteoarthritis. *Exp Ther Med.* **20**, 2631-2638 (2020).

## Figures

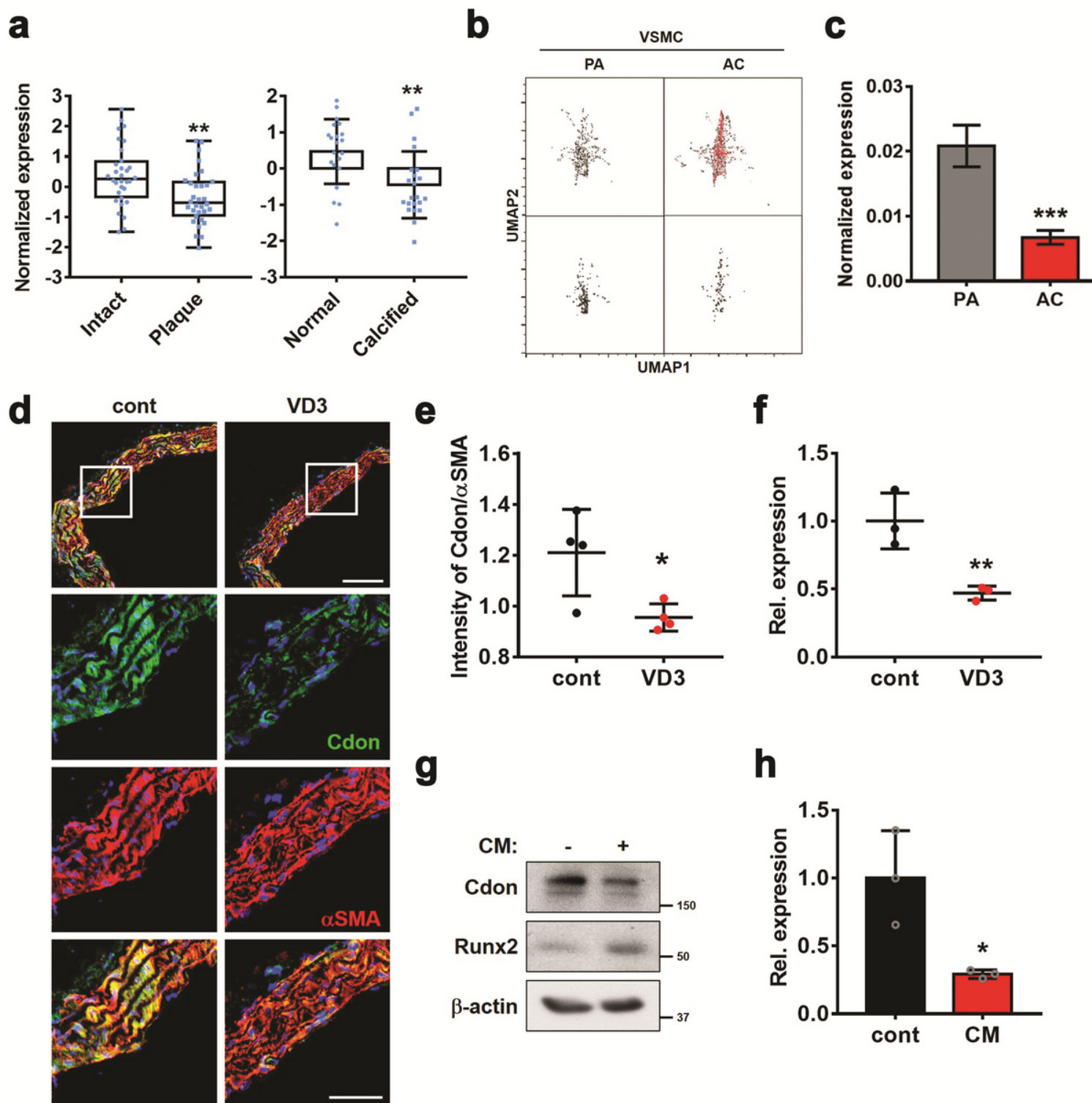
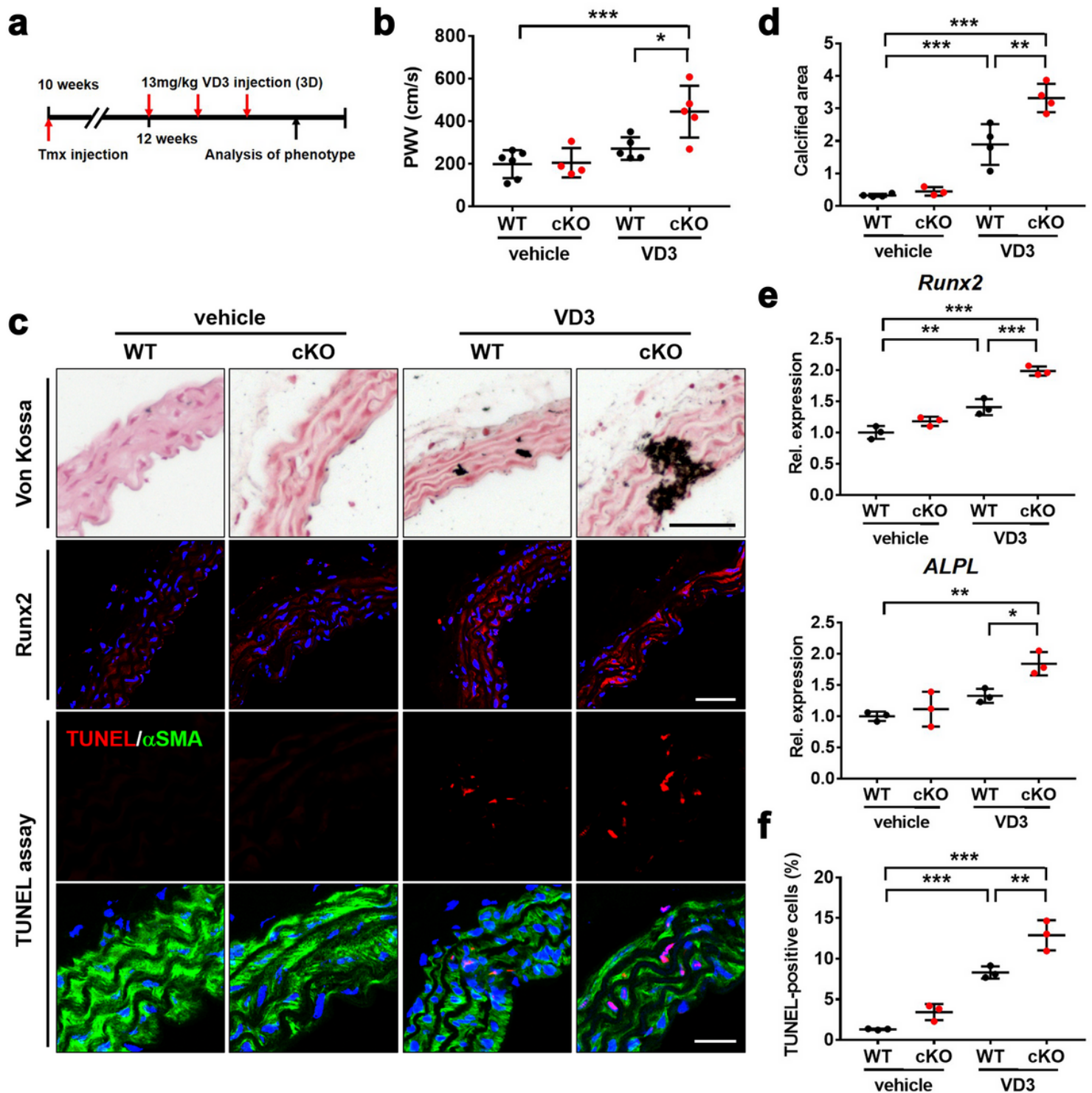


Figure 1

Cdon expression is reduced in calcified aortas.

**(a)** Scatterplots of *Cdon* expression in aortic samples from patients with atherosclerotic plaques (GSE43292, n=32) and calcified aortas (GSE12644 and GSE83453, n=22). Statistical significance is determined with two-tailed Student's t-test. \*\*p<0.01. **(b)** Uniform manifold approximation and projection (UMAP) visualization of VSMCs (Upper box: all genes in VSMCs, bottom box: only *Cdon* expression in VSMCs) in calcified atherosclerotic core plaques (AC) and patient-matched proximal adjacent portions (PA) of carotid artery (GSE159677, n=3). **(c)** *Cdon* expression in PA VSMCs and AC VSMCs (n=3). Statistical significance is determined with two-tailed Student's t-test. \*\*\*p<0.005. **(d)** Representative immunostaining images of *Cdon* and aSMA in aortas injected with vitamin D3 (VD3). Scale bar: 100mm (First) and 50mm (Second). **(e)** Quantification of the intensity of *Cdon* fluorescence normalized by the intensity of aSMA as shown in panel C (n=4). Data represent means  $\pm$ SEM analyzed by Student's t-test. \*p<0.05. **(f)** Relative RNA expression level of *Cdon* in aortic samples from VD3-injected mice (n=3). Data represent means  $\pm$ SEM analyzed by Student's t-test. \*\*p<0.01. **(g)** Immunoblot analysis of VSMCs cultured with calcifying medium (CM). **(h)** The relative RNA expression of *Cdon* in CM-treated VSMCs. Data represent means  $\pm$ SEM analyzed by Student's t-test. \*p<0.05.



**Figure 2**

Cdon deficiency aggravates the aortic stenosis and calcification.

(a) The experimental scheme to induce vascular calcification in WT or Cdon-deficient aortas. cKO mice were generated by tamoxifen (tmx) injection. WT or cKO were injected subcutaneously with vitamin D3 (VD3) for three times as indicated. (b) Echocardiographic parameters for the aortic stenosis: the pulse wave velocity (PWV) in control or VD3-injected WT or cKO mice (n=5). Data represent means  $\pm$  SEM

analyzed by one-way ANOVA test. \* $p < 0.05$ , \*\*\* $p < 0.005$ . (c) Representative images for Von Kossa staining and immunostaining for Runx2 and TUNEL assay in control or VD3-treated WT or cKO aortas. Scale bar: 100mm (Upper), 40mm (Middle), and 20mm (Bottom). (d) Quantification of calcified area in control or VD3-treated aortas as shown in panel C (n=4). Data represent means  $\pm$ SEM analyzed by one-way ANOVA test. \*\* $p < 0.01$ , \*\*\* $p < 0.005$ . (e) Relative RNA expression of osteogenic markers in control or VD3-treated WT or cKO aortas (n=3). Data represent means  $\pm$ SEM analyzed by one-way ANOVA test. \* $p < 0.05$ , \*\* $p < 0.01$ , \*\*\* $p < 0.005$ . (f) Quantification of the number of TUNEL-positive VSMCs in cKO mice with VD3 (n=3) as shown in panel C. Data represent means  $\pm$ SEM analyzed by one-way ANOVA test. \*\* $p < 0.01$ , \*\*\* $p < 0.005$ .

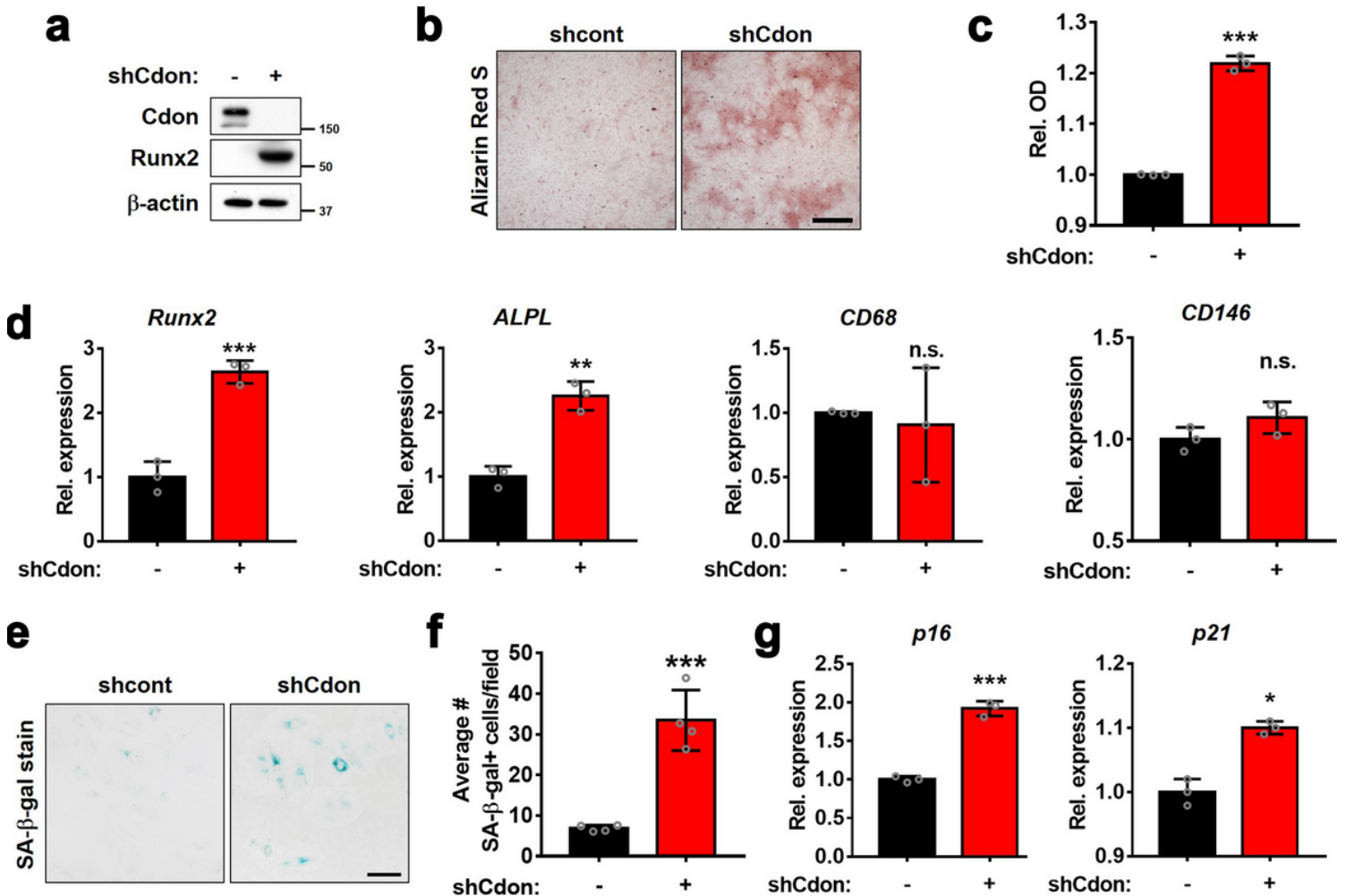


**Figure 3**

Cdon depletion elicits the transition of VSMCs to osteoblast-like cells.

(a) Immunoblot analysis of VSMCs infected with lentivirus expressing control or shCdon. (b) Representative Alizarin Red staining images of shCon- or shCdon-transduced VSMCs. Scale bar: 100mm. (c) Quantification of Alizarin Red staining in VSMCs transduced with shCont or shCdon-lentiviruses. (n=3). Data represent means  $\pm$ SEM analyzed by Student's t-test. \*\*\* $p < 0.005$ . (d) Relative transcript levels of osteogenic markers and foam cell markers in control or Cdon-depleted VSMCs. (n=3). Data represent

means  $\pm$ SEM analyzed by Student's t-test.  $**p < 0.01$ ,  $***p < 0.005$ . (e) Representative images for the senescence associated- $\beta$ -galactosidase (SA- $\beta$ -gal) staining in control or Cdon-deficient VSMCs. Scale bar: 100 $\mu$ m. (f) Quantification of the number of SA- $\beta$ -gal positive cells. (n=4). Data represent means  $\pm$ SEM analyzed by Student's t-test.  $***p < 0.005$ . (g) Relative transcript levels of cellular senescence markers in control or Cdon-deficient VSMCs. (n=3). Data represent means  $\pm$ SEM analyzed by Student's t-test.  $*p < 0.05$ ,  $***p < 0.005$ .

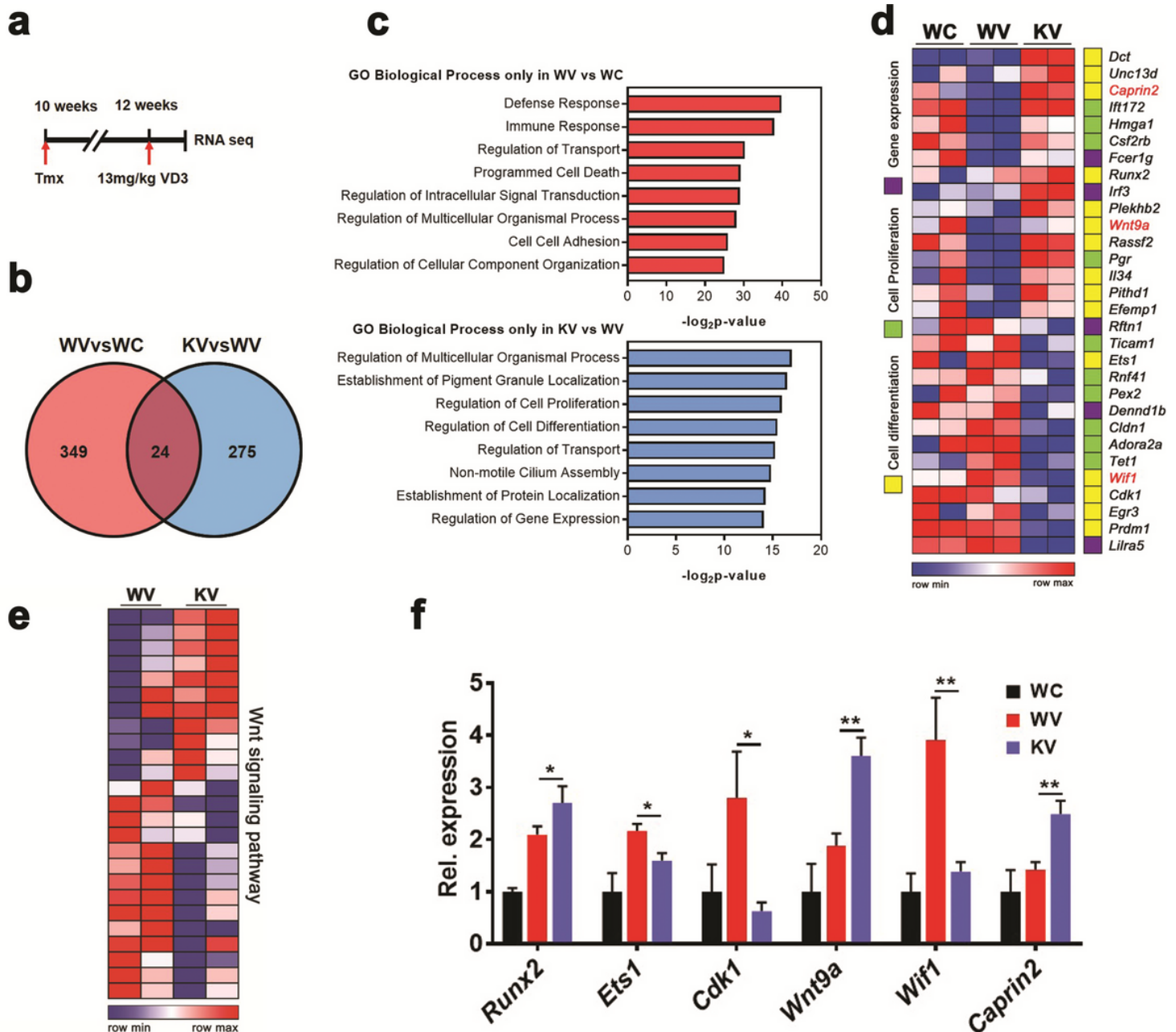
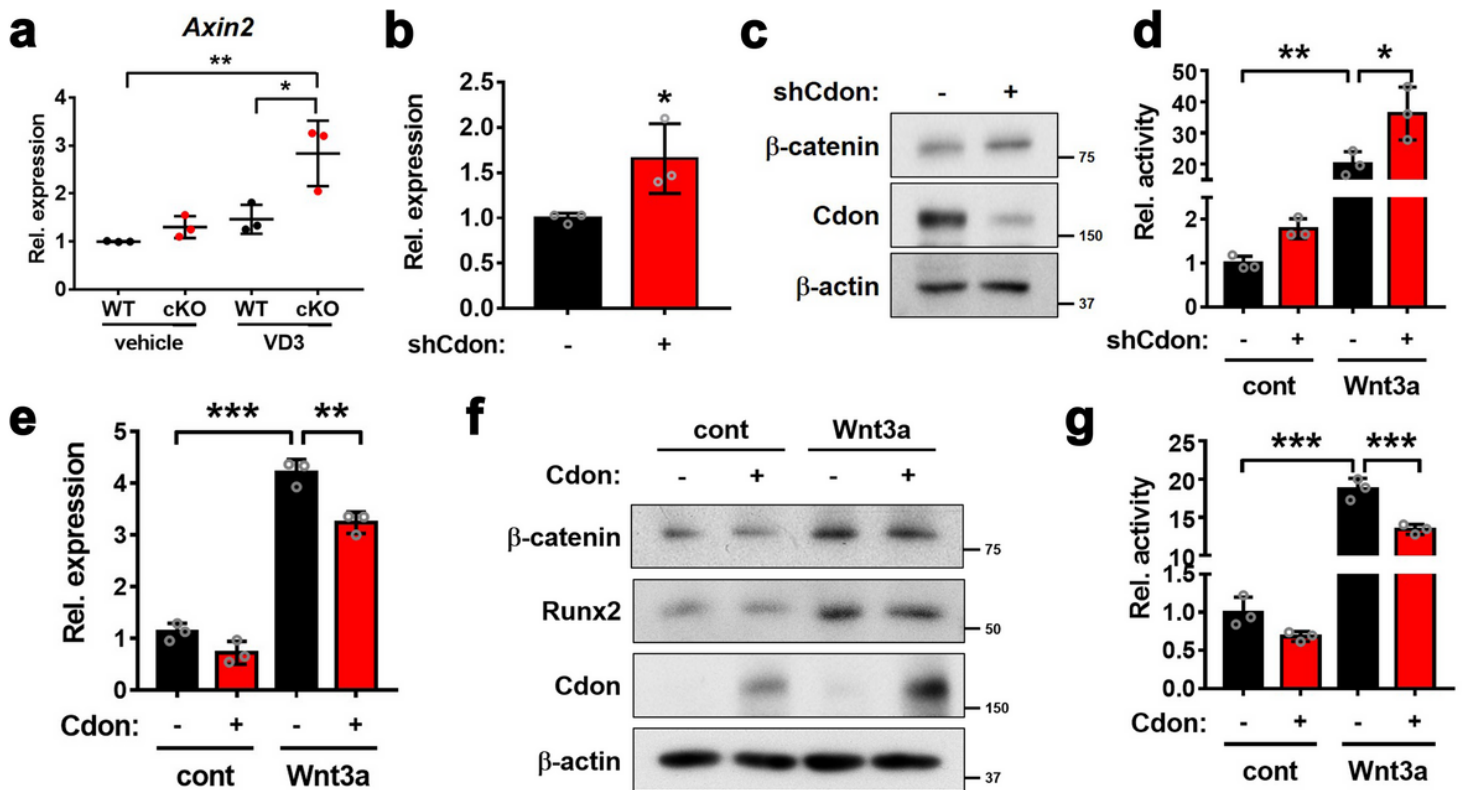


Figure 4

Cdon-deficient aorta displays alterations in genes related to cell proliferation and differentiation accompanied by Wnt signaling components.

(a) The experimental scheme for the RNA-sequencing analysis using RNAs from the aortas of vehicle-treated WT (WC), VD3-treated WT (WV), and VD3-treated cKO (KV) for 1 day. (b) Venn diagram for shared or distinct gene number among the differentially expressed genes in WV vs WC and KV vs WV (n=2, with biological repeat, >1.3 fold, normalized with |RC| log<sub>2</sub> > 2, p < 0.05). (c) Enriched GO terms in biological process term of 349 VD3-mediated unique genes (Upper) or 275 Cdon-dependent VD3-regulated genes (Bottom) by GSEA analysis. (d) The heatmap showing gene expression pattern of three gene sets (Cell Differentiation, Cell Proliferation, and Gene expression). Red letter marks the regulator of Wnt signaling. (e) The comparison of gene expression level implicating Wnt signaling between WV and KV. (f) Relative transcript levels. (n=3). Data represent means ±SEM analyzed by one-way ANOVA test. \*p<0.05, \*\*\*p<0.01.



**Figure 5**

Cdon depleted VSMCs exhibits elevated Wnt signaling.

(a) Relative Axin2 transcript levels in control and VD3-treated aortas. (n=3). Data represent means ±SEM analyzed by one-way ANOVA test. \*p<0.05, \*\*p<0.01. (b) Relative Axin2 transcript level of control or Cdon-deficient VSMCs. (n=3). Data represent means ±SEM analyzed by Student's t-test. \*p<0.05. (c) Immunoblot analysis of control or shCdon-lentiviral infected VSMCs. (d) Top-flash reporter activity of control or Cdon-depleted VSMCs in response to Wnt3a. (n=3). Data represent means ±SEM analyzed by one-way ANOVA. \*p<0.05, \*\*p<0.01. (e) Relative Axin2 expression in control or Cdon-overexpressing VSMCs treated with Wnt3a. (n=3). Data represent means ±SEM analyzed by one-way ANOVA test. \*\*p<0.01, \*\*\*p<0.005. (f) Immunoblot analysis of control or Cdon-overexpressing VSMCs in response to

Wnt3a. (g) The top-flash reporter activity of control or Cdon-overexpressing VSMCs, in response to Wnt3a. (n=3). Data represent means  $\pm$ SEM analyzed by Student's t-test and one-way ANOVA. \*\*\*p<0.005.

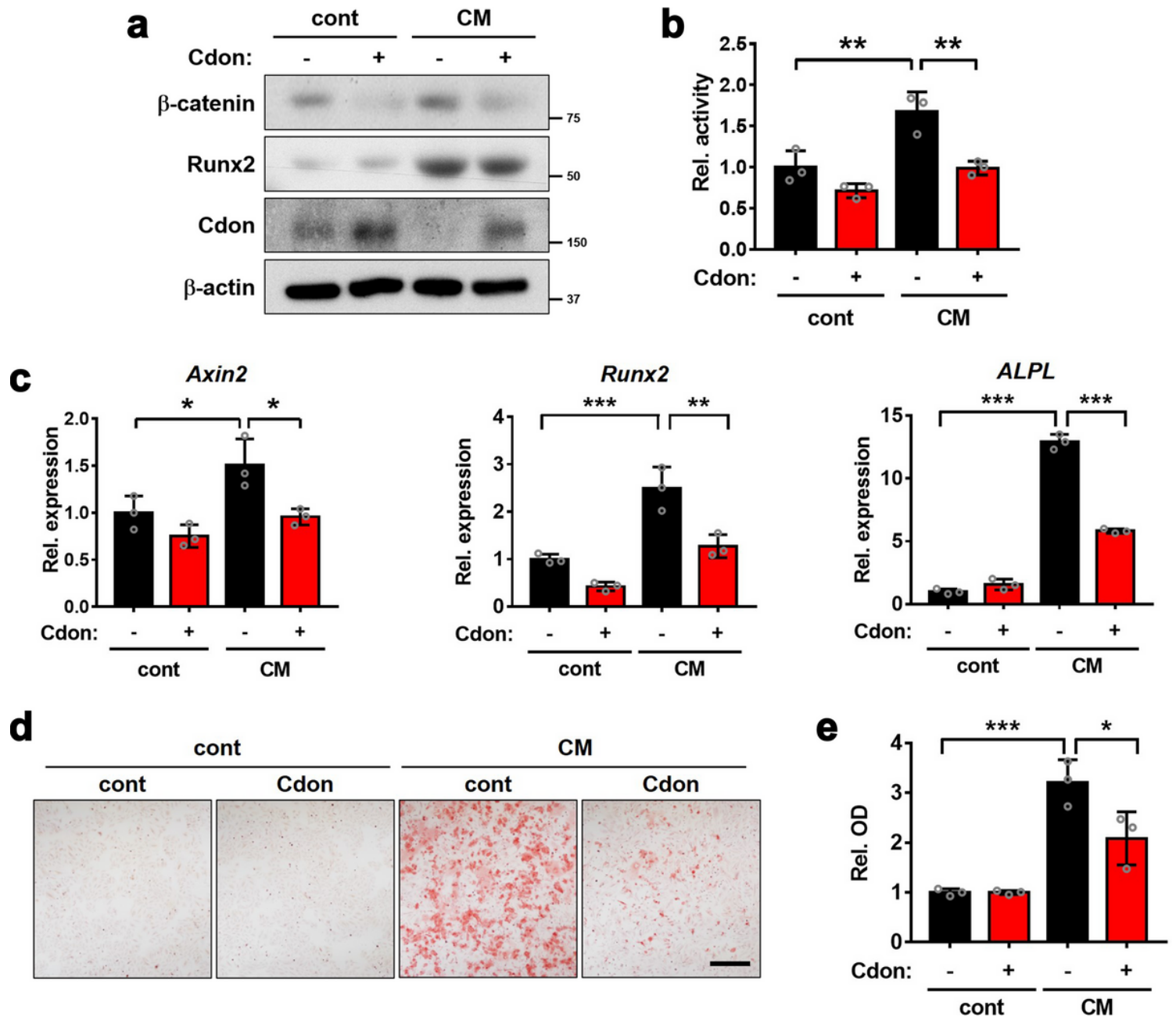


**Figure 6**

Cdon overexpression attenuates the osteogenic conversion of VSMCs in response to CM.

(a) Immunoblot analysis of control or Cdon-overexpressing VSMCs in response to CM. (b) The Top-flash reporter activity in control or Cdon-overexpressing VSMCs in response to CM. (n=3). Data represent means  $\pm$ SEM analyzed by one-way ANOVA test. \*\*p<0.01. (c) Relative RNA expression of Axin2, Runx2, and ALPL in control or Cdon-overexpressing VSMCs treated with CM. (n=3). Data represent means  $\pm$ SEM analyzed by one-way ANOVA test. \*p<0.05, \*\*p<0.01, and \*\*\*p<0.005. (d) Alizarin Red staining images of control or Cdon-overexpressing VSMCs in response to CM. Scale bar: 100mm. (e) Quantification of the

Alizarin Red staining in VSMCs. (n=3). Data represent means  $\pm$ SEM analyzed by one-way ANOVA test. \* $p < 0.05$ , \*\*\* $p < 0.005$ .

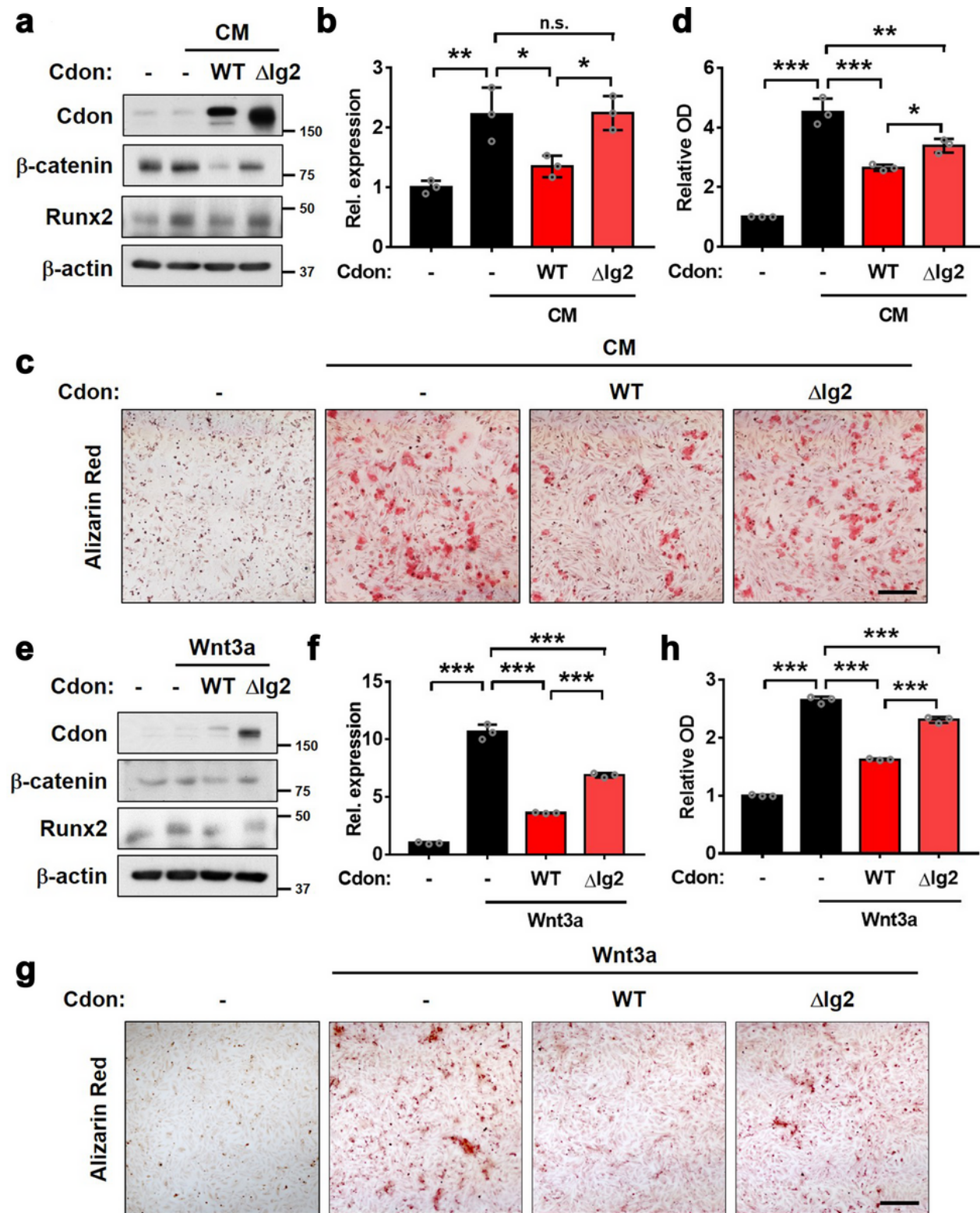


Figure 7

The deletion of Ig2 domain of Cdon fails to block the VSMC osteogenic conversion.

(a) Immunoblot analysis of VSMCs expressing control, full-length Cdon or Ig2 domain-deleted Cdon (DIg2) treated with vehicle or CM. (b) Relative Axin2 expression in control, Cdon or DIg2-expressing VSMCs in response to CM. (n=3). Data represent means  $\pm$ SEM analyzed by one-way ANOVA. n.s.=not significant, \* $p$ <0.05, \*\* $p$ <0.01, \*\*\* $p$ <0.005. (c) Alizarin Red staining of control, Cdon or DIg2-expressing VSMCs in response to CM. Scale bar: 100 $\mu$ m. (d) Quantification of Alizarin Red staining. (n=3). Data represent means  $\pm$ SEM analyzed by one-way ANOVA test. \* $p$ <0.05, \*\*\* $p$ <0.005. (e) Immunoblot analysis of VSMCs expressing control, full-length Cdon or Ig2 domain-deleted Cdon (DIg2) treated with vehicle or Wnt3a. (f) Relative Axin2 expression in control, Cdon or DIg2-expressing VSMCs in response to Wnt3a. (n=3). Data represent means  $\pm$ SEM analyzed by one-way ANOVA. \*\*\* $p$ <0.005. (g) Alizarin Red staining of control, Cdon or DIg2-expressing VSMCs in response to Wnt3a. Scale bar: 100 $\mu$ m. (h) Quantification of Alizarin Red staining. (n=3). Data represent means  $\pm$ SEM analyzed by one-way ANOVA test. \*\*\* $p$ <0.005.

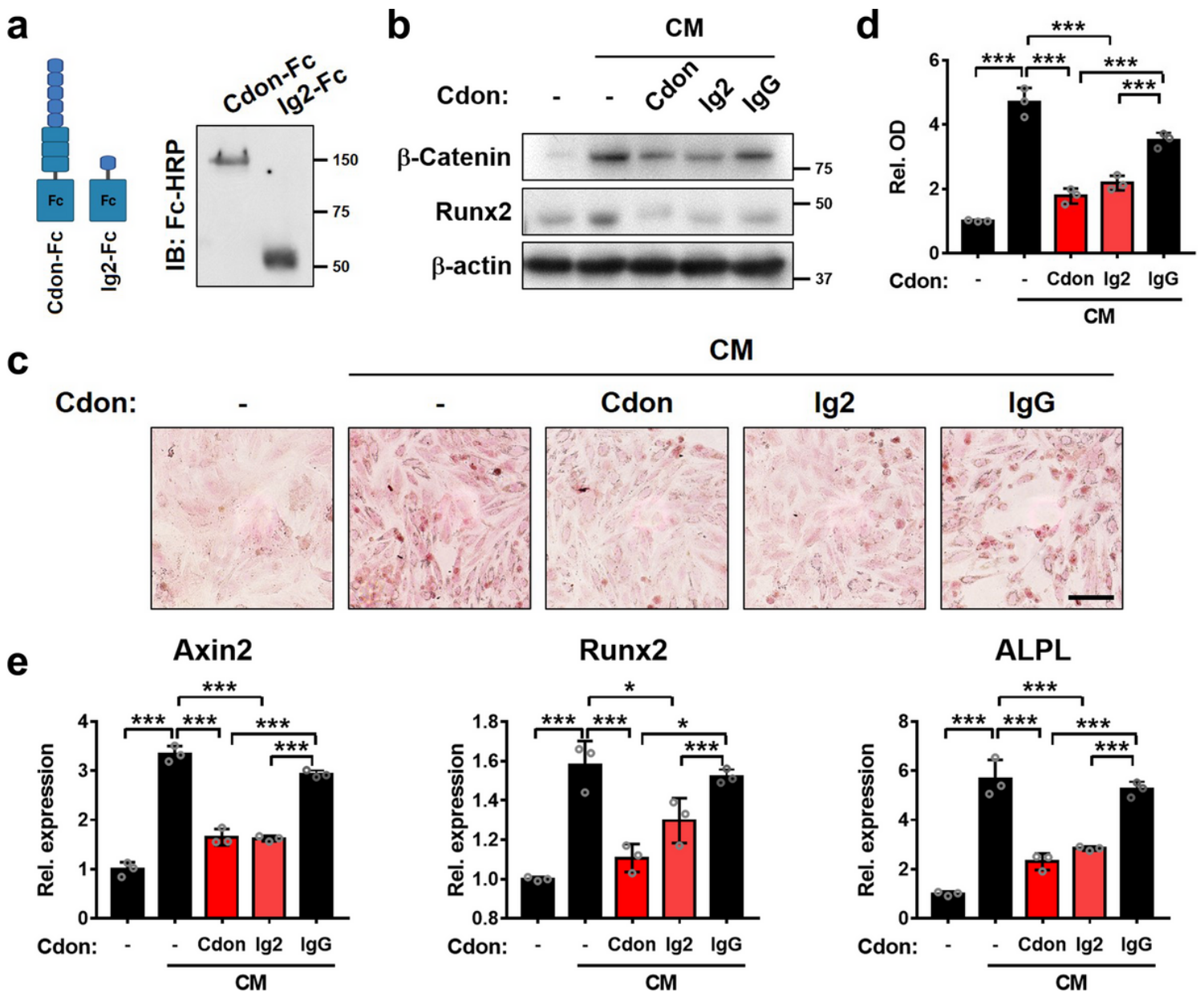


Figure 8

The Ig2 domain of Cdon is sufficient to attenuate the osteogenic conversion of VSMCs.

**(a)** Immunoblot analysis of Cdon-Fc (the entire Cdon ectodomain fused to Fc) and Ig2-Fc (Ig2 domain fused to Fc) purified from cell supernatants. **(b)** Immunoblot analysis of VSMCs treated with CM or purified proteins. IgG serves as a control. **(c)** Alizarin Red staining images of VSMCs treated with control or CM in combination of Cdon-Fc, Ig2-Fc or IgG. Scale bar=100mm. **(d)** Quantification of Alizarin Red staining. (n=3). Data represent means  $\pm$ SEM analyzed by one-way ANOVA test. **(e)** Relative transcript levels of Axin2, Runx2 and ALPL in VSMCs treated with control or CM in combination of Cdon-Fc, Ig2-Fc or IgG.

## Supplementary Files

This is a list of supplementary files associated with this preprint. Click to download.

- [Supplementarymaterial.docx](#)
- [SFig1.tif](#)
- [SFig2.tif](#)
- [SFig4.tif](#)
- [SFig3.tif](#)
- [SFig5.tif](#)